HemaSphere
Powered by EHA

EHA EUROPEAN HEMATOLOGY ASSOCIATION

Letter
OPEN ACCESS

Control of Systemic Iron Homeostasis by the 3' Iron-Responsive Element of Divalent Metal Transporter 1 in Mice

Elisabeth Tybl[1], Hiromi Gunshin[2†], Sanjay Gupta[1], Tomasa Barrientos[3], Michael Bonadonna[1,4], Ferran Celma Nos[5], Gael Palais[1], Zoubida Karim[6], Mayka Sanchez[5], Nancy C. Andrews[7], Bruno Galy[1]

Correspondence: Bruno Galy (e-mail: b.galy@dkfz.de).

Tight control of intestinal iron absorption is required to avoid both iron insufficiency and excess.[1] Dietary nonheme iron is taken up by absorptive enterocytes via the apical iron transporter DMT1 (a.k.a. SLC11A2),[2–4] and transferred into the circulation by ferroportin (FPN, a.k.a. SLC40A1), with the help of a ferroxidase, hephaestin (HEPH).[1] FPN activity is controlled by the liver hormone hepcidin,[1] but DMT1 seems regulated locally via mechanisms operating within enterocytes.[5,6] *DMT1* messenger ribonucleic acid (mRNA) exists in four isoforms that differ in their 5' and 3' ends.[7] 3' end diversity results from alternative usage of splicing and polyadenylation sites and yields isoforms that either contain or lack a conserved iron responsive element (IRE) in their 3' untranslated region (UTR). IRE-containing isoforms are predominant in duodenal enterocytes.

IREs are stem-loop structures that interact with iron regulatory proteins (IRPs, a.k.a. ACO1 and IREB2) in iron-depleted cells.[1] IRP binding to multiple IREs in the 3'-UTR of the transferrin receptor 1 (*TFRC*) mRNA limits its degradation by Regnase-1 (a.k.a. ZC3H12A).[8] The presence of an IRE-like motif in *DMT1* suggests that *DMT1* could be regulated by IRPs, similar to *TFRC*. However, the single *DMT1* IRE contains an additional 3'-bulge in its upper stem, and *DMT1* mRNA seems to lack a Regnase-1 binding site.[9] Importantly, DMT1 expression only responds to iron fluctuation in a subset of cell lines,[10,11] and the *DMT1* 3'IRE failed to exhibit iron-dependent regulation in reporter assays.[11] Furthermore, *Dmt1* transcription is controlled by HIF2α (a.k.a. EPAS1),[5,6] which itself is regulated by IRPs,[1] confounding the study of specific functions of the *Dmt1* 3'IRE.[12] Here, we address the role of this ribonucleic acid (RNA) motif using a mouse model with selective disruption of the *Dmt1* 3'IRE.

We established a mouse line lacking the 5' stem, the apical loop and part of the 3' stem of the *Dmt1* 3'IRE (Fig. 1A–D and Supplemental Materials and Methods, http://links.lww.com/HS/A91). Mutagenesis of the *Dmt1* 3'IRE impairs IRP binding. Importantly, all four DMT1 transcripts are adequately expressed in homozygous mutant mice, including those that bear the dysfunctional IRE (Supplemental Figure 1, http://links.lww.com/HS/A91). The resulting allele (designated $Dmt1^{IRE\Delta}$) is inherited in Mendelian proportions (Supplemental Table 1, http://links.lww.com/HS/A91). Both $Dmt1^{IRE\Delta/\Delta}$ males and females are viable and fertile and exhibit normal posture and activity patterns. Blood cell parameters (Supplemental Table 2, http://links.lww.com/HS/A91) are globally preserved during postnatal growth (2 weeks of age, during a period of high iron demand), early adulthood (3 months of age) and advanced age (9 months). A flow cytometry analysis did not reveal any abnormality of terminal erythroid differentiation in young adults (Supplemental Figure 2, http://links.lww.com/HS/A91). The mean weight is slightly higher in 2-week-old $Dmt1^{IRE\Delta/\Delta}$ pups but later is comparable to $Dmt1^{IRE+/+}$ littermates (Supplemental Table 3, http://links.lww.com/HS/A91). Spleen, liver, kidney, and heart weights were unchanged (Supplemental Table 3, http://links.lww.com/HS/A91). These data show that while *Dmt1* is essential during perinatal life and critical for erythroid iron acquisition,[2,3] its 3'IRE is not required under standard laboratory conditions and appears to be dispensable for normal hematopoiesis.

Interestingly, 2-week-old $Dmt1^{IRE\Delta/\Delta}$ male mice display a 40% reduction in serum iron levels, and a decrease in transferrin saturation (Fig. 1E). In spite of the hypoferremia, hepcidin concentration, which is low during postnatal growth, is not affected (Fig. 1F). Similarly, both hepatic and splenic iron stores are small and remain indistinguishable from wild-type animals

[1]German Cancer Research Center (DKFZ), Division of Virus-Associated Carcinogenesis (F170), Heidelberg, Germany
[2]Department of Nutrition, University of Massachusetts, Amherst, Massachusetts, United States
[3]Duke University School of Medicine, Department of Orthopedic Surgery, Durham, North Carolina, United States
[4]Biosciences Faculty, University of Heidelberg, Heidelberg, Germany
[5]Iron Metabolism: Regulation and Diseases Group, Department of Basic Sciences, Faculty of Medicine and Health Sciences, Universitat Internacional de Catalunya (UIC), Barcelona, Spain
[6]INSERM U1149, Paris Diderot University, Sorbonne Paris Cité, and Laboratory of Excellence GR-Ex, Paris, France
[7]Duke University School of Medicine, Department of Pharmacology and Cancer Biology and Department of Pediatrics, Durham, North Carolina, United States.
†Deceased
This work was supported by the Howard Hughes Medical Institute (N.C.A.) and a grant from the Deutsche Forschungsgemeinschaft to B.G. (GA2075/5-1).
The authors have no conflicts of interest to disclose.
Supplemental Digital Content is available for this article.

HemaSphere (2020) 4:5(e459). http://dx.doi.org/10.1097/HS9.0000000000000459.
Received: 22 April 2020 / Accepted: 26 June 2020

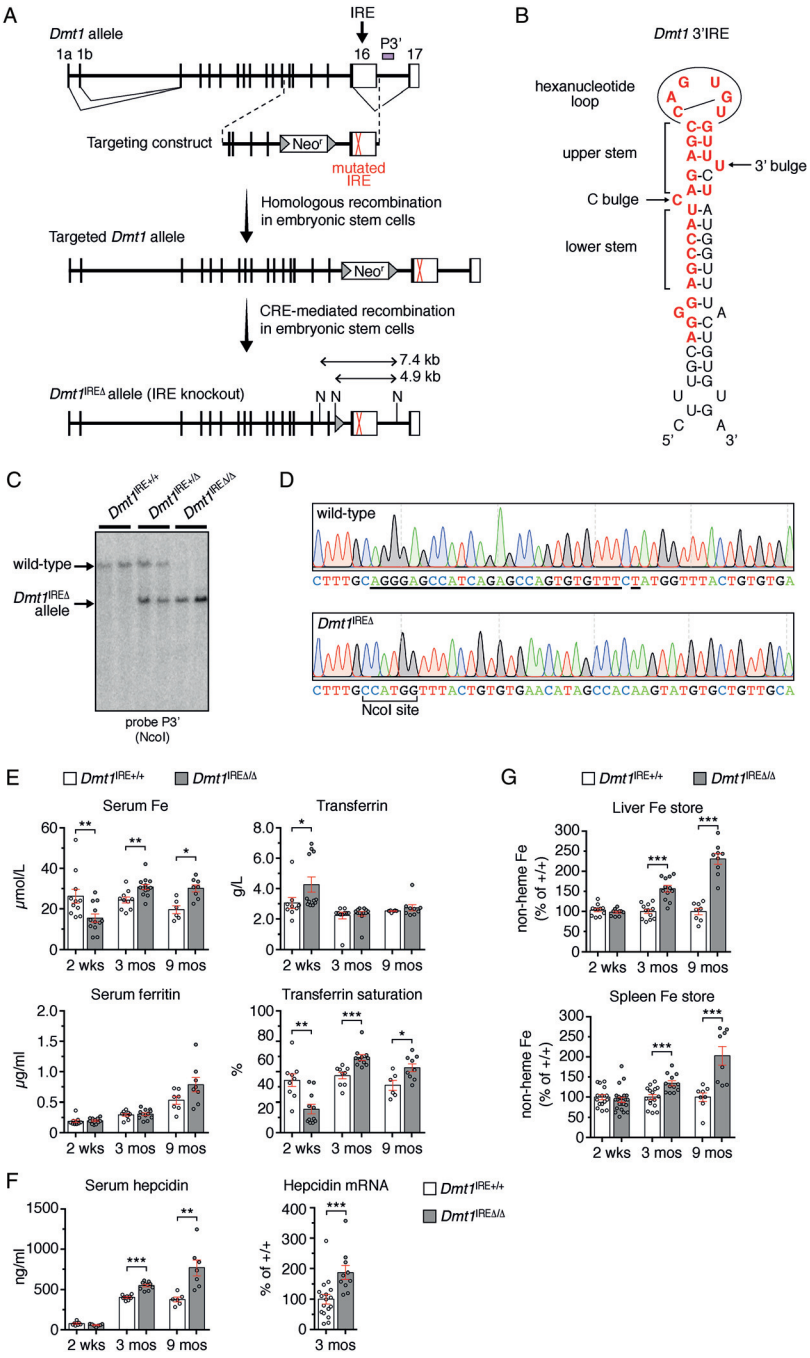

Figure 1. Disruption of the *Dmt1* 3'IRE decreases serum iron levels during early life but leads to hyperferremia in adulthood. (A) The *Dmt1* locus comprises 18 exons. The first exon is transcribed from 2 alternative promoters termed 1a and 1b, respectively. 3' end diversity results from alternative splicing and alternative usage of polyadenylation sites: inclusion of exon 16 gives rise to *Dmt1* mRNA isoforms bearing the 3'UTR IRE; non-IRE isoforms arise from the joining of a splice donor located upstream of the IRE within exon 16 with the splice acceptor of exon 17. The IRE stem-loop was mutagenized using a targeting construct encompassing exons 12 to 16; a CD neomycin (Neo) resistance cassette (indicated Neo^r) flanked with *LoxP* sites (depicted by grey triangles) was inserted into intron 15 and served as a selection marker. The *Dmt1* IRE was replaced by the mutated IRE through homologous recombination in embryonic stem cells. The CD-Neo cassette was subsequently removed via transient expression of CRE recombinase to obtain the *Dmt1*$^{IRE\Delta}$ allele. (B) Schematic representation of the murine *Dmt1* IRE stem-loop structure. The bases highlighted in red are deleted in the *Dmt1*$^{IRE\Delta}$ allele. (C) Southern-blot analysis of the *Dmt1* locus in *Dmt1*$^{IRE+/+}$, *Dmt1*$^{IRE+/\Delta}$, and *Dmt1*$^{IRE\Delta/\Delta}$ mice with a 3' external probe (P3') after digestion of genomic deoxyribonucleic acid with NcoI, indicated N in (A). (D) Total RNA from wild-type (top) and mutant (bottom) littermates was reverse transcribed and the IRE region of the *Dmt1* mRNA was PCR amplified (Supplemental Table 4, http://links.lww.com/HS/A91) and sequenced. The electropherograms confirm proper mutagenesis of the 3'IRE of the *Dmt1* mRNA. The nucleotides deleted in the wild-type IRE are underlined. The NcoI site created in the mutated IRE is shown. (E) Serum iron parameters were assessed in male mice at 2 weeks (2 wks), 3 months (3 mos) and 9 months (9 mos) of age (6–13 male mice per group). (F) Serum hepcidin concentration (left) and liver hepcidin mRNA levels (right) in 3-month-old male mice. (G) The liver and splenic iron stores were determined in male mice (8–22 mice per group) at different stages of life, as in (E). The results are expressed as percentage of wild-type littermates for each range of age. Note that the hepatic and splenic iron stores of 2 week-old mice are low compared to adults (liver: ~ 100 ± 32 mg nonheme iron/g of dry tissue in 2-week old wild-type males vs 279 ± 51 and 357 ± 62 mg/g at 3 and 9 months of age, respectively; spleen: 227 ± 14 mg/g in 2 week-old wild-type males vs 1927 ± 119 and 3887 ± 744 mg/g at 3 and 9 months of age, respectively). Histograms display averages ± SEM. p: Student *t*-test (*: $p < 0.05$; **: $p < 0.01$; ***: $p < 0.001$). CD = cytidine deaminase, IRE = iron responsive element, mRNA = messenger ribonucleic acid, RNA = ribonucleic acid.

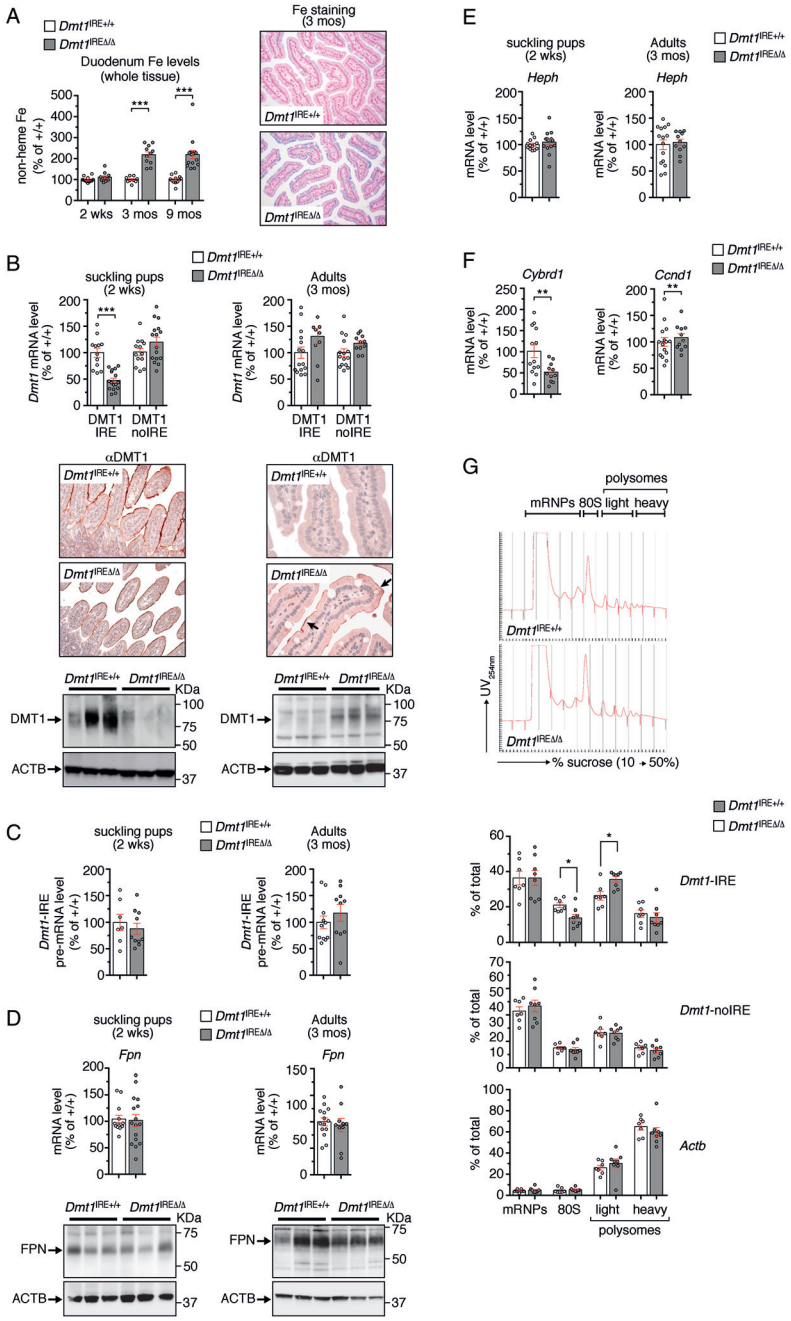

Figure 2. The *Dmt1* 3'IRE exerts divergent effects on intestinal DMT1 expression in postnatal vs adult animals. (A) Left: Duodenal nonheme iron levels were analyzed in male mice at different stages of life as in Figure 1E (9–15 mice per group). Right: Perl's staining in the duodenum of 3-month old male mice showing iron deposition in mucosal cells (counterstain: nuclear fast red). (B) Top: qPCR analysis of *Dmt1* mRNA levels in the duodenum of 2 week- (left) vs 3 month- (right) old mice using IRE vs non-IRE-specific primers (Supplemental Table 4, http://links.lww.com/HS/A91). The data display transcript levels as percentage of control (ie, $Dmt1^{IRE+/+}$) after calibration to *Actb* (n = 9–16 mice per group); similar results were obtained when using *Gapdh* and/or *Tubb5* as standard (not shown). Middle panels: immunostaining of DMT1 in the duodenum (counterstain: hematoxylin); a higher magnification is presented for adult tissues because the DMT1 signal (arrows) is fainter than in suckling pups. Bottom: representative western-blot analysis of DMT1 in whole duodenal extracts. (C) qPCR analysis of *Dmt1* pre-mRNA levels in 2-week- vs 3-month-old male mice, after calibration to the *Actb* pre-mRNA (similar results were obtained after calibration of *Gapdh* pre-mRNA, not shown). (D) qPCR (top) and western-blot (bottom) analysis of ferroportin expression in the duodenum of mice at 2 weeks (left) vs 3 months (right) of age. For western blotting (B and D), ACTB was used as loading control. In (A) and (B), pictures were acquired with a DM5000 microscope equipped with a DFC420C camera and a 10× (A), 20× (B, 2 weeks) or 40× (B, 3 months) objectives, and were processed using the Leica Application Suite (Leica Biosystems, Wetzlar, Germany). (E) qPCR analysis of *Heph* mRNA levels in the duodenum of 2 week- vs 3-month old mice. (F) qPCR analysis of HIF2-target genes in the duodenum of 3-month-old animals. The qPCR data in (D) to (F) display transcript levels as percentage of control (ie, $Dmt1^{IRE+/+}$) after calibration to *Actb* (similar results were obtained after calibration on *Gapdh* and/or *Tubb5*, not shown). (G) Duodenal scrapings from 3-month old mice were resolved through linear 10% to 50% sucrose density gradients and fractions were collected with constant UV recording (top). Fractions corresponding to untranslated mRNA (mRNP: messenger ribonucleoprotein), monosomes (80S), as well as light and heavy polysomes were collected. The amount of *Dmt1* (IRE and non-IRE isoforms) and *Actb* mRNAs in those fractions was determined by qPCR. The histograms (bottom) represent mRNA levels across the fractions as a percentage (mean ± SEM, n = 7–8) of the sum of all fractions. Histograms display averages ± SEM. p: Student *t*-test (*: $p < 0.05$; **: $p < 0.01$; ***: $p < 0.001$). IRE = iron responsive element, mRNA = messenger ribonucleic acid, RNA = ribonucleic acid.

(Fig. 1G). In contrast to suckling pups, 3 month-old *Dmt1*$^{IRE\Delta/\Delta}$ males exhibit high serum iron and transferrin saturation values (Fig. 1E) and an increase in tissue iron stores (Fig. 1G), accompanied by an augmentation of serum hepcidin (Fig. 1F, left) attributable to stimulation of the hepcidin transcript in liver (Fig. 1F, right). Nine-month-old *Dmt1*$^{IRE\Delta/\Delta}$ males display a comparable hyperferremia and a trend towards high serum ferritin (Fig. 1E), associated with hepatic and splenic iron loading (Fig. 1G). *Dmt1*$^{IRE\Delta/\Delta}$ female mice show a similar, albeit less pronounced iron phenotype (Supplemental Figure 3, http://links.lww.com/HS/A91) at 2 weeks and 3 months. Enlargement of tissue iron stores in *Dmt1*$^{IRE\Delta/\Delta}$ adults is not associated with aberrantly high expression of mRNAs encoding known iron import or sequestration genes, nor with marked suppression of transcripts coding for iron export molecules (Supplemental Figure 4, http://links.lww.com/HS/A91), suggesting that tissue iron loading is secondary to the elevation of serum iron rather than a consequence of aberrant iron management in liver and spleen cells.

Iron dyshomeostasis in *Dmt1*$^{IRE\Delta/\Delta}$ mice could result from altered intestinal iron absorption.[1,4] At 2 weeks of age, duodenal nonheme iron levels are indistinguishable from wild type (Fig. 2A). However, *Dmt1*$^{IRE\Delta/\Delta}$ pups exhibit a selective downregulation of the *Dmt1*-IRE mRNA isoform, associated with a decrease in total DMT1 protein levels and reduced DMT1 immunostaining at the apical membrane of enterocytes (Fig. 2B). The downregulation of the *Dmt1*-IRE mRNA is largely posttranscriptional, since *Dmt1*-IRE pre-mRNA levels are not significantly altered (Fig. 2C). This is in agreement with the predicted role of 3'UTR IREs, based on analogy to *TFRC*, where IRP binding decreases mRNA decay.[1,8] Considering that FPN protein and *Heph* mRNA levels are not reduced (Fig. 2D and E), the hypoferremia in *Dmt1*$^{IRE\Delta/\Delta}$ pups could be explained by downregulation of intestinal DMT1 expression. During adulthood, *Dmt1*$^{IRE\Delta/\Delta}$ mice exhibit an approximately 2-fold increase in enterocyte iron accumulation (Fig. 2A), associated with normal expression of FPN and *Heph* (Fig. 2D and E). In contrast to its partial suppression in *Dmt1*$^{IRE\Delta/\Delta}$ pups, IRE-containing *Dmt1* mRNA is expressed at nearly wild-type levels in adult intestine (Fig. 2B). It is unlikely that this is due to compensatory stimulation of *Dmt1* transcription by HIF2.[5,6] Indeed, mRNA levels of *Fpn* and *Ccnd1*, both HIF2-target genes, are not increased (Fig. 2D and F). *Cybrd1*, another HIF2-target, appears to be repressed (Fig. 2F). Moreover, *Dmt1* pre-mRNA levels are unchanged (Fig. 2C). Hence, the 3'IRE of *Dmt1* exerts a positive effect on intestinal DMT1 expression during the postnatal period of growth but not during adult life. This age-dependent effect of the *Dmt1* 3'IRE appears to be tissue-specific. While it is also observed in heart, it is not detected in spleen or kidney (Supplemental Figures 4 and 5, http://links.lww.com/HS/A91). Surprisingly, while *Dmt1*$^{IRE\Delta/\Delta}$ adults express nearly wild-type levels of *Dmt1*-IRE mRNA, duodenal DMT1 protein expression is increased (Fig. 2B). Although we cannot exclude changes in protein turnover,[13] we speculated that disruption of the *Dmt1* 3'IRE could alter mRNA translation. Supporting this notion, we observed a significant shift of the *Dmt1*-IRE mRNA isoform from monosomes to polysomes (Fig. 2G), suggesting that the *Dmt1* 3'IRE partially represses *Dmt1* mRNA translation in the adult duodenum. As we did not detect obvious signs of altered urinary iron excretion (not shown), the relatively mild iron accumulation in *Dmt1*$^{IRE\Delta/\Delta}$ animals could reflect a modest increase in dietary iron absorption secondary to intestinal DMT1 protein upregulation, leading to progressive accretion of iron in the body over time.

The functionality of the *DMT1* 3'IRE has been questioned. Although it exhibits weaker affinity for IRPs than other IREs, the *DMT1* 3'IRE does bind IRP1 in the native cellular environment.[14] Our work confirms that the 3'IRE of *Dmt1* plays a role in controlling DMT1 expression and systemic iron homeostasis and reveals an age-dependent switch in its activity. During postnatal growth, the *Dmt1* 3'IRE promotes intestinal DMT1 expression and secures iron sufficiency; in adulthood, it suppresses DMT1 and prevents systemic iron loading.

Surprisingly, the IRE of *Dmt1* seems to influence different aspects of RNA fate in the intestine at different times – abundance and stability during early life and mRNA translation in adulthood. The molecular details of this age-related switch in the function of the *Dmt1* 3'IRE remain unknown. 3'UTR based-gene regulation is often mediated through the binding of proteins and/or microRNAs to specific RNA sequences and/or structures. We speculate that factors with tissue- and/or age-specific activity or expression might influence the way the *Dmt1* 3'IRE modulates DMT1 levels. Of note, single 3'IREs have been identified in other transcripts, including the *Cdc14a* and *Pfn2* mRNAs.[1] Like *DMT1*, the regulation of those mRNAs appears to be cell type-specific and different from the regulation of *TFRC*. Whether those other single 3'IREs regulate gene expression through a mechanism similar to the *DMT1* 3'IRE remains to be determined.

It is well established that *Dmt1* regulation in the duodenal mucosa is strongly dependent on HIF2.[15] In that context, the precise role of the age-dependent switch in the activity of the *Dmt1* 3'IRE remains to be defined. The *Dmt1* 3'IRE may contribute to maintaining baseline homeostasis of immature intestinal absorption early in life, whereas, in adulthood, the 3'IRE may help to fine-tune DMT1 expression to avoid excessive iron assimilation.

Acknowledgements

We thank Sandro Altamura (University of Heidelberg, Germany) for fruitful discussions. We are grateful to the staff of the DKFZ animal facility for their dedicated care of the animals. We thank the "Plateforme de Biochimie" at the "Centre de Recherche sur l'Inflammation" (Paris, France) for their measurement of serum parameters. This work was supported by the Howard Hughes Medical Institute (NCA) and a grant from the Deutsche Forschungsgemeinschaft to B.G. (GA2075/5-1).

References

1. Muckenthaler MU, Rivella S, Hentze MW, et al. A red carpet for iron metabolism. *Cell.* 2017;168:344–361.
2. Gunshin H, Mackenzie B, Berger UV, et al. Cloning and characterization of a mammalian proton-coupled metal-ion transporter. *Nature.* 1997; 388:482–488.
3. Fleming MD, Trenor CC, Su MA, et al. Microcytic anaemia mice have a mutation in Nramp2, a candidate iron transporter gene. *Nat Genet.* 1997;16:383–386.
4. Shawki A, Anthony SR, Nose Y, et al. Intestinal DMT1 is critical for iron absorption in the mouse but is not required for the absorption of copper or manganese. *Am J Physiol Gastrointest Liver Physiol.* 2015;309: G635–G647.
5. Shah YM, Matsubara T, Ito S, et al. Intestinal hypoxia-inducible transcription factors are essential for iron absorption following iron deficiency. *Cell Metab.* 2009;9:152–164.
6. Mastrogiannaki M, Matak P, Keith B, et al. HIF-2alpha, but not HIF-1alpha, promotes iron absorption in mice. *J Clin Invest.* 2009;119: 1159–1166.

7. Hubert N, Hentze MW. Previously uncharacterized isoforms of divalent metal transporter (DMT)-1: implications for regulation and cellular function. *Proc Natl Acad Sci USA.* 2002;99:12345–12350.
8. Yoshinaga M, Nakatsuka Y, Vandenbon A, et al. Regnase-1 maintains iron homeostasis via the degradation of transferrin receptor 1 and prolyl-hydroxylase-domain-containing protein 3 mRNAs. *Cell Rep.* 2017;19:1614–1630.
9. Mino T, Murakawa Y, Fukao A, et al. Regnase-1 and roquin regulate a common element in inflammatory mRNAs by spatiotemporally distinct mechanisms. *Cell.* 2015;161:1058–1073.
10. Wardrop SL, Richardson DR. The effect of intracellular iron concentration and nitrogen monoxide on Nramp2 expression and non-transferrin-bound iron uptake. *Eur J Biochem.* 1999;263:41–49.
11. Gunshin H, Allerson CR, Polycarpou-Schwarz M, et al. Iron-dependent regulation of the divalent metal ion transporter. *FEBS Lett.* 2001; 509:309–316.
12. Galy B, Ferring-Appel D, Becker C, et al. Iron regulatory proteins control a mucosal block to intestinal iron absorption. *Cell Rep.* 2013;3: 844–857.
13. Foot NJ, Leong YA, Dorstyn LE, et al. Ndfip1-deficient mice have impaired DMT1 regulation and iron homeostasis. *Blood.* 2011;117:638–646.
14. Connell GJ, Danial JS, Haastruthers CX. Evaluation of the iron regulatory protein-1 interactome. *Biometals.* 2018;31:139–146.
15. Schwartz AJ, Das NK, Ramakrishnan SK, et al. Hepatic hepcidin/intestinal HIF-2α axis maintains iron absorption during iron deficiency and overload. *J Clin Invest.* 2019;129:336–348.